

# Power Doppler Ultrasound Evaluation of the Shear Rate and Shear Stress Dependences of Red Blood Cell Aggregation

Guy Cloutier,\* *Member, IEEE*, Zhao Qin, Louis-Gilles Durand, *Senior Member, IEEE*, and Beng Ghee Teh

**Abstract**—The use of power Doppler ultrasound at 10 MHz is evaluated as a method to study the shear rate and the shear stress dependences of red blood cell aggregation. This evaluation was based on six *in vitro* experiments conducted in a 1.27-cm diameter tube under steady flow conditions. Porcine whole blood was circulated in the flow model at flow rates ranging between 125 to 1500 ml/min (mean shear rate across the tube ranging between 6 and 74 s<sup>-1</sup>). For each flow condition, the variation of the Doppler power across the tube and the velocity profile were measured by moving the Doppler sample volume across the tube diameter. For each radial position, the shear rate within the Doppler sample volume was also determined by considering the radial power pattern of the ultrasound beam. To estimate the shear stress within the Doppler sample volume, the apparent viscosity of blood samples withdrawn from the flow model was measured for each experiment. The variation of the Doppler power as a function of the shear rate within the sample volume showed a rapid reduction of the power between 1 and 5 s<sup>-1</sup>, a transition region between 5 and 10 s<sup>-1</sup>, and a very slow reduction beyond 10 s<sup>-1</sup>. Little variation of the Doppler power was measured for shear stress higher than 2 dyn/cm<sup>2</sup>. The maximum Doppler power for all flow rates was usually found near the center of the tube. Based on the ultrasonic scattering models, which predict that the Doppler power is related to the volume square of the scatterers, the method described in the present study showed a very high sensitivity to the presence of red blood cell aggregation for shear rates below 10 s<sup>-1</sup>.

## I. INTRODUCTION

RED blood cell aggregation is a reversible physiological phenomenon that constitutes one of the most important factors responsible for the non-Newtonian properties of normal human blood. The mechanisms of rouleaux formation and dissociation are very complex and depend on the physiochemical properties of several plasma proteins, the intrinsic properties of the red blood cells, and the mechanical properties of the flow [1], [2]. Rouleaux of red cells are normally easily broken down by an external force and they are formed again when the external force is reduced or removed. Under flowing condi-

Manuscript received July 7, 1995; revised December 22, 1995. This work was supported by the Fonds de la Recherche en Santé du Québec under a research scholarship, the Medical Research Council of Canada under grant MA-12 491, the Whitaker Foundation, Pennsylvania, USA, and the Heart and Stroke Foundation of Quebec. *Asterisk indicates corresponding author.*

\*G. Cloutier is with the Laboratoire de Génie Biomédical, Institut de Recherches Cliniques de Montréal, 110 avenue des Pins Ouest, Montréal, Québec Canada H2W 1R7 (e-mail: cloutig@ircm.umontreal.ca).

Z. Qin, L.-G. Durand, and B. G. Teh are with the Laboratoire de Génie Biomédical, Institut de Recherches Cliniques de Montréal, Montréal, Québec H2W 1R7 Canada.

Publisher Item Identifier S 0018-9294(96)03180-1.

tions, the formation, and break-up of aggregates are governed by the shear stress acting on the red cells. Under pathological conditions, it is believed that an elevated level of red cell aggregation may contribute to the initiation, development, and aggravation of cardiovascular disease [3]–[7].

The feasibility of using ultrasound to detect red cell aggregation induced by dextran and fibrinogen was first demonstrated by Shung and Reid [8]. Later, it was postulated that the echogenicity of blood in large abdominal veins of dogs was due to the presence of red blood cell aggregation [9]. Other studies hypothesized red cell aggregation to be a cause of the smoke-like spontaneous echo contrast observed *in vivo* in low flow conditions [10]–[14]. In parallel to these clinical studies, experimental investigations aimed at elucidating factors affecting the backscattered power under flowing conditions of red blood cell aggregates were reported [15]–[22]. Static methods were also proposed to study red cell aggregation with ultrasound [23]–[25]. It was demonstrated in these studies that the echogenicity of blood depends on the shear rate, the hematocrit, the frequency of the ultrasound beam, the stoppage of the flow, the pulsation rate, and the concentration of dextran, fibrinogen, and other plasma proteins. Among all these factors, the shear rate (or shear stress) is the most important parameter affecting blood echogenicity under flowing conditions. Since the volume of the red cell aggregates depends on the shear rate and since the ultrasound backscattering coefficient from blood is theoretically proportional to the square of the volume of the scatterers [26], a high sensitivity of the technique to the presence of red cell aggregation is anticipated.

An exponentially decaying relationship between the A-mode echo amplitude measured at the center of a tube and the mean shear rate across the tube was first demonstrated by Sigel *et al.* [9], [27]. A reduction of the amplitude of the echo by approximately 31 dB was found for mean shear rates varying between zero (five minutes after flow stoppage) and 41 s<sup>-1</sup> [9]. The relationship between the shear rate and blood echogenicity was later studied by many groups. However, with the exception of the study performed by Shehada *et al.* [22], no measurement of the shear rate at the site of the blood echogenicity evaluation was performed. In other experiments [9], [15]–[17], [20], [27], the echogenicity was compared to the cross-sectional mean shear rate estimated assuming Poiseuille flow, while it was expressed as a function of the shear rate derived from the Womersley model in the study by Kim *et al.* [18]. In the present study, the relationship

between the mean shear rate within the Doppler sample volume and porcine whole blood echogenicity was determined with a vertical steady flow loop model for shear rates varying between approximately  $1\text{--}100\text{ s}^{-1}$ . The relationship between the Doppler power and the shear stress acting on red cells was also evaluated.

## II. MATERIALS AND METHODS

### A. Flow Loop Model and Experimental Design

Experiments were performed in a vertical steady flow loop model at room temperature (Fig. 1). The main flow conduit was a thin-wall heat-shrinkable transparent Kynar tubing having an inside diameter, when not heated, of 1.27 cm. The inlet length of the tube between the top reservoir and the site of Doppler recordings was sufficient ( $l = 57\text{ cm}$ ) to have a fully developed laminar flow for all flow rates used in the study. A reservoir of one liter (bottom reservoir in Fig. 1) allowed filling of the model with blood or a water-glycerol solution. Continuous mixing of the solution was performed by a magnetic stirrer. A peristaltic pump (lung-heart pump, Sarns Inc.) circulated the fluid from the bottom reservoir to the top reservoir. High impedance small openings were located between the top reservoir and the entrance of the vertical tube to reduce the oscillations produced by the pump. A constant pressure head was maintained and residual oscillations in the flow were eliminated by the overflow conduit located between the top and bottom reservoirs. Since the height difference between both reservoirs was constant, a valve was used to adjust the flow rate, which was continuously monitored with a cannulating type flow probe (Carolina Medical Electronics, model SF625) connected to an electromagnetic blood flowmeter (Carolina Medical Electronics, Cliniflow II, model FM701D).

The first series of measurements were performed with a mix of water-glycerol and 2 g/liter of superfine Sephadex particles (Sigma Chemical) to verify the presence of a fully developed laminar flow in the model. A volume of 60% saline and 40% glycerol was used to mimic the viscosity of whole blood. This Newtonian blood mimicking fluid was selected because it provides a parabolic velocity profile if the flow is effectively fully developed. The presence of a parabolic flow profile was verified by moving the position of the Doppler sample volume across the tube. The details of the method used to evaluate the velocity profiles are given below.

A total of six experiments were performed with porcine whole blood to measure the shear dependence of red cell aggregation using power Doppler ultrasound. Porcine whole blood was selected because of the requirement of a large quantity of blood, and because of its red cell aggregation properties which were recently shown to be similar to those of normal human blood [28]. The fresh blood collected from an abattoir was adjusted to 40% hematocrit by remixing the plasma, white cells, and red cells separated by sedimentation. At the beginning and at the end of each experiment, the hematocrit obtained by microcentrifugation (Haemofuge, Heraeus Instruments), the temperature, the pH (Sentron, model

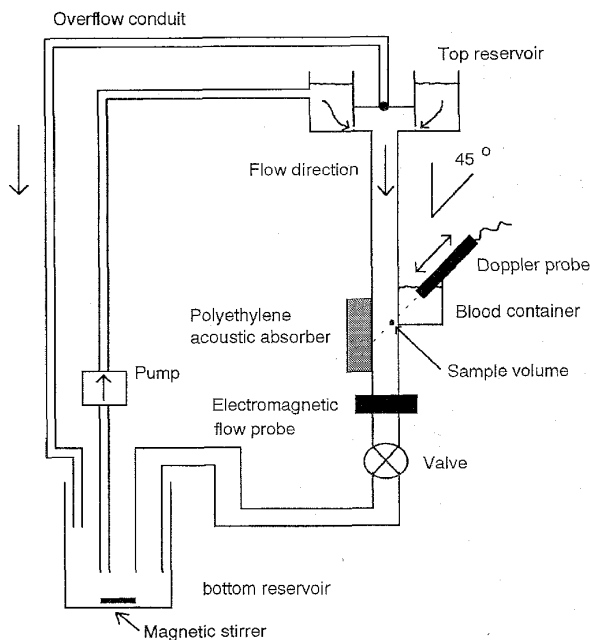


Fig. 1. Schematic representation of the steady flow model.

1001), the partial dissociation shear rate (laser light erythro-aggregometer, Regulest, France), and the apparent viscosity at shear rates between 288 and  $1\text{ s}^{-1}$  (Brookfield cone-plate viscometer, model LVDVIII-CP-42) were measured. The partial dissociation shear rate, which represents the shear rate needed for partially disrupting the rouleaux of red cells, was obtained from the erythro-aggregometer using the method described by Donner *et al.* [29]. A blood sample of 1.5 ml was withdrawn from the flow model and the dissociation shear rate was measured from the variation of the light intensity scattered by the blood sample submitted to a Couette flow at shear rates between 720 and  $6\text{ s}^{-1}$ .

### B. Doppler Data Acquisition and Spectral Analysis

Doppler measurements were performed with a pulsed-wave 10-MHz Doppler system developed at Baylor College of Medicine, Houston, TX. A pulse-repetition frequency (PRF) of 19.5 kHz was used. The cut-off frequency of the high-pass clutter filter was set at 3 Hz. The angle between the tube axis and the nonfocused Doppler transducer was maintained at  $45^\circ$ . The transducer, having a  $3\text{ mm} \times 3\text{ mm}$  dimension, was positioned visually in line with the center of the tube. The Doppler in-phase ( $I$ ) and quadrature ( $Q$ ) components and the electromagnetic flowmeter output were digitized at sampling rates of 19.5 kHz and 195 Hz, respectively, for 10 seconds. The Doppler signals digitized with a Data Translation board (model DT-2821G-SE) were processed with autoregressive spectral modeling over temporal windows of 10 ms. A time interval of 10 ms separated each window. For each recording, 1000 Doppler spectra and a mean spectrum were computed. The mean spectrum was normalized by the frequency response of the Doppler flowmeter to compensate for its limited frequency

bandwidth. A flat bandwidth between 3 Hz and half of the pulse repetition frequency (9.75 kHz) was then obtained. The optimal number of poles of the autoregressive estimation algorithm was determined by using the “Akaike’s information criterion.”

### C. Experimental Evaluation of the Velocity Profile

All experiments were performed at flow rates of 125, 250, 500, 750, 1000, 1250, and 1500 ml/min in order to cover a range of shear rates within the Doppler sample volume from approximately 1 to 100 s<sup>-1</sup>. The velocity profile was obtained for each flow rate by moving the transducer by steps of 0.5 mm. Twenty-five measurements were performed across the tube diameter. A Brüel and Kjaer audio analyzer (model 2012) was used to monitor the Doppler frequency shift when adjusting the position of the probe. The minimum shear rate for a given experiment was obtained at the center of the tube and at a flow rate of 125 ml/min while the maximum shear rate was found close to the wall at a flow rate of 1500 ml/min.

For each position of the sample volume across the tube diameter, the Doppler mean velocity of the forward flow component of the mean spectrum was evaluated as follows:

$$V_d = \frac{c}{2f_o \cos \theta} \times \frac{\sum_{f_k=-BW}^{BW} f_k P(f_k)}{\sum_{f_k=-BW}^{BW} P(f_k)} \quad (1)$$

where  $c$  is the speed of ultrasound in blood (1570 m/s),  $f_o$  the ultrasound carrier frequency,  $\theta$  the Doppler angle,  $\pm BW$  the higher and lower frequencies of the -5-dB bandwidth of the dominant frequency peak, and  $P(f_k)$  the power in a bandwidth  $\Delta f = 19$  Hz (19.5 kHz/1024 samples) centered at the frequency  $f_k$ . The mean frequency was computed within  $\pm BW$  to eliminate the bias attributable to the noisy frequency components of the mean spectrum.

Since the maximum velocity at the center of the tube was not necessarily measured, the alignment of the experimental velocities with the tube axis and the extrapolation of the positions of the zero velocity values at the wall were not straightforward. No determination of the center of the tube was attempted from the experimental data because of the possible variance in the velocity estimate and also because of the limited resolution of the sampled data (0.5 mm  $\times$  sin $\theta$  in the radial direction of the tube). A second order least-square model defined as

$$V(x) = a_0 + a_1 x + a_2 x^2 \quad (2)$$

was fitted to the experimental velocity data. In (2),  $a_i$  are the parameters of the model and  $x$  is the relative position of the Doppler sample volume across the tube. The position corresponding to the maximum of (2) allowed the determination of the center axis of the tube. The left and right locations of the wall were obtained by adding  $\pm R$  to the center position, where  $R = 6.35$  mm is the radius of the tube.

### D. Cross-Sectional Distribution of the Doppler Power

For each position of the Doppler sample volume across the tube, the Doppler power of the mean spectrum was computed by

$$P = \frac{1}{N} \sum_{f_k=-(PRF/2)+1}^{+PRF/2} P(f_k) \quad (3)$$

where  $N = 1024$  is the number of samples between  $\pm PRF/2$ . Since the size of the Doppler sample volume and the attenuation of the transmitted ultrasound signal influence the power of the backscattered echoes, both parameters were carefully controlled in the flow model. Misinterpretations of the red blood cell aggregation characteristics would be possible without using the following experimental approach.

The position of the transducer was moved instead of that of the gated echoes to maintain a constant sample volume size of 3.7 mm<sup>3</sup> at -3 dB. The distance between the face of the transducer and the recording sites was fixed at 1.9 cm (far-field) for all measurements (assuming the speed of sound is 1570 m/s in blood) by using the same delay of 24  $\mu$ s between transmitted and gated echoes. In order to maintain a constant sound attenuation when moving the transducer, the Doppler probe was submerged in blood in a container (Fig. 1) to provide similar attenuating properties between the Doppler probe and the location of the sample volumes. Mixing of blood in this container was performed regularly to avoid sedimentation. The attenuation due to the wall of the tube was constant for all measurements and did not contribute to the variation of the Doppler power.

### E. Shear Rate within the Doppler Sample Volume

To determine the mean shear rate within the Doppler sample volume, the experimental velocities  $V_d$  and the extrapolated zero velocity values at the wall were fitted to the power law model [30, p. 322]

$$v(r) = v_{\max} [1 - (r/R)^n] \quad (4)$$

where  $v_{\max}$  is the maximum centerline velocity,  $r$  the distance from the center of the tube,  $R$  the radius of the tube, and  $n$  the power law exponent. For a parabolic flow velocity profile,  $n = 2$  and it is greater than two for a blunt profile.

The shear rate  $\gamma(r)$  across the tube is, by definition, the rate of change  $\partial v(r)/\partial r$  of the velocity across the tube. By computing the derivative of (4), the shear rate  $\gamma(r)$  was estimated by

$$\gamma(r) = n v_{\max} r^{(n-1)} / R^n. \quad (5)$$

The mean shear rate averaged across the area of the tube was determined using

$$\bar{\gamma} = \frac{2v_{\max}}{R} \left( \frac{n}{n+1} \right). \quad (6)$$

As schematized in Fig. 2, the mean shear rate within the Doppler sample volume  $\gamma(r)_{sv}$  was estimated by weighting

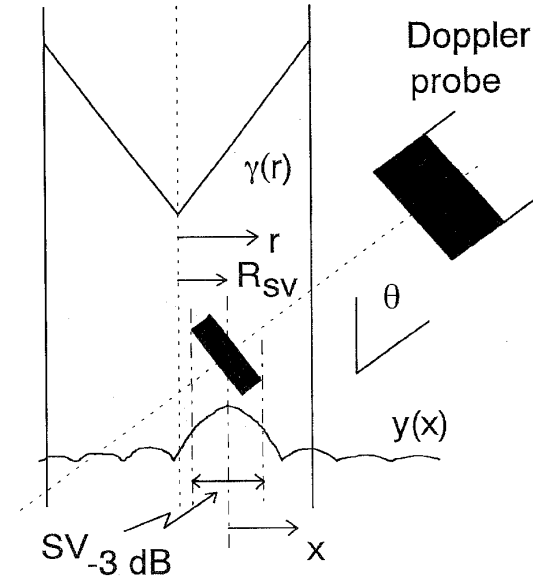


Fig. 2. Illustration describing the method used to evaluate the mean shear rate within the Doppler sample volume.

the shear rate  $\gamma(r)$  with a theoretical function of the radial ultrasonic beam power pattern in the far-field [31]. This function for a rectangular transducer was shown to be described by

$$y(\alpha) = \sin^2(\alpha\pi)/(\alpha\pi)^2 \quad (7)$$

where  $\alpha$  is the radial position. The normalized function  $y(\alpha)$  has a value of one for  $\alpha = 0$  and zero for  $\alpha = \pm 1, \pm 2$ , etc. Two assumptions were made in the present study for estimating  $\gamma(r)_{sv}$ . First, the projection of the power distribution of the three-dimensional sample volume on the radial axis of the tube had the form of the function  $y(\alpha)$ , and second, the beam power variation in the axial direction of the sample volume was minimum.

Based on these hypotheses, the projection of the sample volume at  $-3$  dB ( $SV_{-3dB}$ ) on the radial axis of the tube was determined by

$$SV_{-3dB} = SV_{\text{radial}} \cos \theta + SV_{\text{axial}} \sin \theta \quad (8)$$

where  $SV_{\text{radial}}$  (2.34 mm) and  $SV_{\text{axial}}$  (0.86 mm) are the diameter of the Doppler sample volume at  $-3$  dB in the radial and axial directions. Since the beam profile  $y(0.443) = 0.5$  ( $-3$  dB), the parameter  $\alpha$  of (7) was substituted by  $0.443x/(SV_{-3dB}/2)$ , where  $x$  is the radial distance from the position of the Doppler sample volume. The mean shear rate within the sample volume  $\gamma(r)_{sv}$  was estimated by

$$\gamma(r)_{sv} = \frac{\sum_{x=-\infty}^{\infty} \gamma(R_{sv} + x)y(x)}{\sum_{x=-\infty}^{\infty} y(x)} \quad (9)$$

where  $R_{sv}$  is the position of the sample volume within the tube.

#### F. Shear Stress within the Doppler Sample Volume

The sliding motion among fluid layers results in a force exerted on each of the layers. In the case of flowing blood in a tube, the force acting on the red cells is the shear stress  $\tau(r)$  given by  $\tau(r) = \mu(\gamma(r)) \times \gamma(r)$ , where  $\mu$  is the apparent viscosity of blood that varies with the shear rate  $\gamma(r)$ . The shear stress acting on the red cells located within the Doppler sample volume,  $\tau(r)_{sv}$ , was estimated by

$$\tau(r)_{sv} = \mu(\gamma(r)_{sv}) \times \gamma(r)_{sv}. \quad (10)$$

To determine the apparent viscosity  $\mu(\gamma)$  at a specific shear rate  $\gamma = \gamma(r)_{sv}$ , the power law model [32]

$$\mu(\gamma) = k\gamma^{m-1} \quad (11)$$

where  $k$  and  $m$  are the parameters of the model, was fitted to the experimental curve relating the apparent viscosity to the shear rate. This curve was determined experimentally with the cone-plate blood viscometer between 288 and  $1 \text{ s}^{-1}$ . The apparent viscosity at the shear rate  $\gamma(r)_{sv}$  was determined from the power law model because only a limited number of apparent viscosity was measured.

#### G. Volumetric Flow Comparison

To assess the reliability of the Doppler velocity profiles, the volumetric flow obtained with the electromagnetic flowmeter was compared with that estimated with the Doppler method. According to [30, p. 323], the Doppler volumetric flow was estimated from

$$Q = \frac{\pi R^2 v_{\text{max}}^n}{n+2} \quad (12)$$

where  $R$ ,  $v_{\text{max}}$ , and  $n$  are the parameters of the power law model described in (4). A first-order least-square model was used to obtain the relationship between the electromagnetic and Doppler volumetric flow estimates.

### III. RESULTS

The first series of measurements were performed with Sephadex particles suspended in a mixture of 60% water and 40% glycerol at a flow rate of approximately 1500 ml/min. The results of Fig. 3 show the experimental velocity measurements and the velocity function obtained from (4). A sound velocity of 1650 m/s was used in (1) to relate the Doppler frequency shifts to the red blood cell velocities ( $0.6 \times 1480$  m/s which is the speed of sound in water +  $0.4 \times 1904$  m/s which is the velocity in glycerol at room temperature [33]). The apparent viscosity of the Newtonian solution was 4.6 cP. A parabolic velocity profile was obtained ( $n = 2.08$ ) which suggests that the entrance length was sufficient and the flow was laminar (Reynolds number = 854).

The hematocrit, pH, temperature, and the partial dissociation shear rate of the red blood cell aggregates were measured at the beginning and at the end of each experiment performed with porcine whole blood. Little variation was observed in each experiment for all parameters. The results expressed in term of mean  $\pm$  one standard deviation (SD) were  $39.8 \pm$

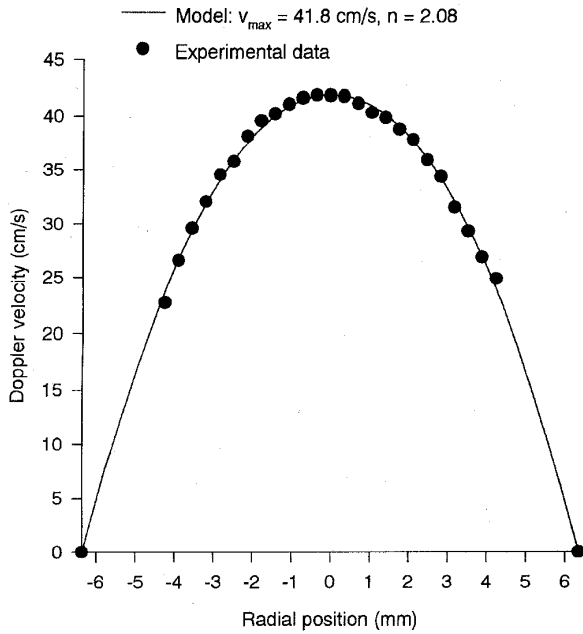


Fig. 3. Experimental velocity measurements across the tube and power law model described by (4).  $V_{max}$  and  $n$  are the best fit parameters of the model. The experiment was performed with a mix of 60% saline water, 40% glycerol, and 2 g/liter of Sephadex superfine particles at a flow rate of 1500 ml/min.

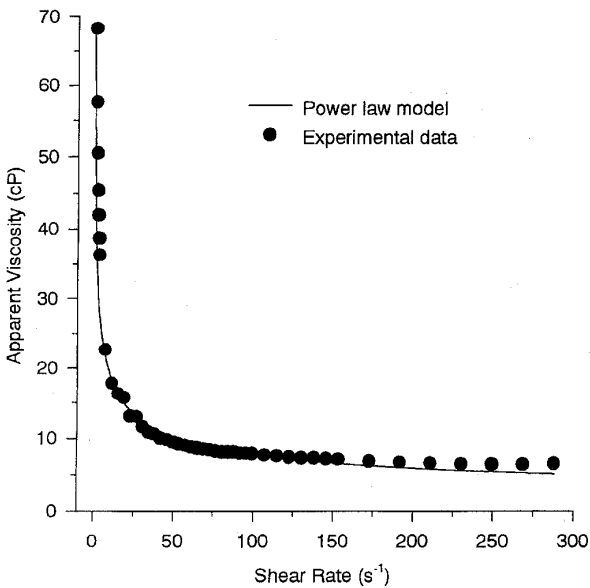


Fig. 4. Example of the relationship between the apparent viscosity and the shear rate obtained from one porcine whole blood sample. The power law model described by (11) is also plotted with the experimental results.

0.2% for the hematocrit,  $7.22 \pm 0.08$  for the pH,  $25 \pm 3^\circ\text{C}$  for the temperature, and  $42 \pm 8 \text{ s}^{-1}$  for the partial dissociation shear rate. An example of the apparent viscosity expressed as a function of the shear rate, with the power law model fitted to the data (11), is shown in Fig. 4.

Examples from one experiment of the Doppler velocity, the Doppler power, the fitted power law velocity model  $v(r)$  (4),

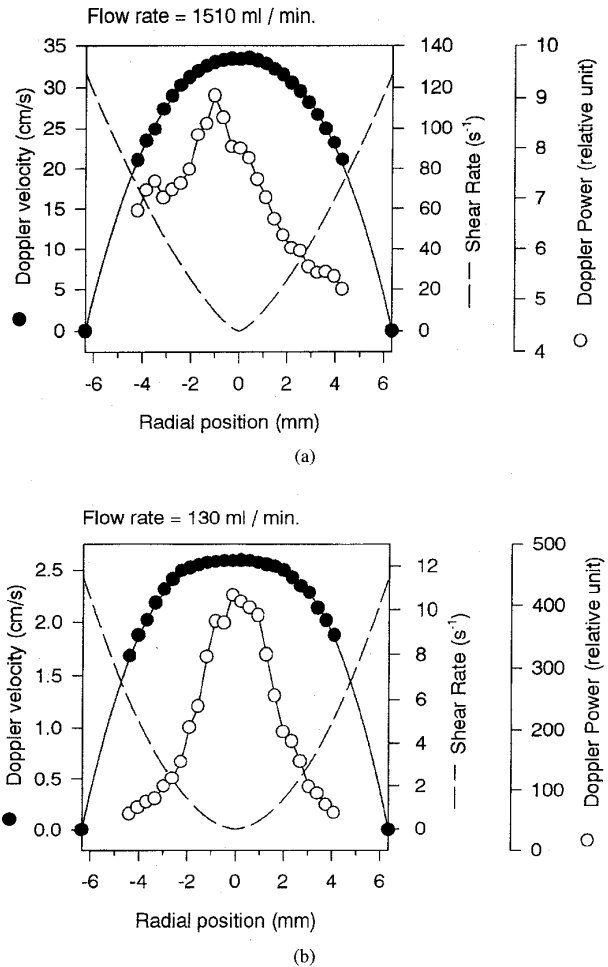


Fig. 5. Examples of the Doppler velocity (black circles), the Doppler power (hollow circles), the fitted power law velocity model  $v(r)$  (full line), and the shear rate model  $\gamma(r)$  (dashed line) obtained from one experiment performed by circulating porcine whole blood in the model at flow rates of (a) 1510 and (b) 130 ml/min.

and the shear rate model  $\gamma(r)$  (5) are shown in Fig. 5 for flow rates of 1510 and 130 ml/min. Similar power Doppler variations were observed for all other flow rates. The power was usually minimum close to the wall and maximum near the center of the tube. Table I summarizes the values of the mean power and the power ratio (maximum/minimum power) across the tube for all flow rates tested. A 17.3 fold increase in the mean power (12.4-dB variation) was found when varying the flow rate from 1505 to 129 ml/min. The power ratios across the tube also increased as the flow rate decreased. A power ratio of 5.8 (7.6 dB) was observed at a flow rate of 129 ml/min while a ratio of 1.7 (2.3 dB) was found at 1505 ml/min.

The reliability of the velocity profiles was assessed by comparing the Doppler volumetric flow with that measured with the electromagnetic flowmeter. As shown in Fig. 6, a good coefficient of determination ( $r^2 = 0.948$ ) was obtained between both measurements. However, the Doppler method underestimated the volumetric flow for all flowrates. Table II

TABLE I

MEAN POWER AND POWER RATIO BETWEEN THE MAXIMUM AND MINIMUM POWER ACROSS THE TUBE AS A FUNCTION OF THE FLOW RATE. ALL RESULTS ARE EXPRESSED IN TERMS OF MEAN  $\pm 1$  STANDARD DEVIATION. THE FLOW RATES WERE MEASURED WITH AN ELECTROMAGNETIC BLOOD FLOWMETER. ALL MEASUREMENTS WERE REPEATED OVER SIX EXPERIMENTS WITH THE EXCEPTION OF THE RESULTS AT 1505 ml/min, SINCE ONLY THREE EXPERIMENTS WERE AVAILABLE

| Flow Rate (ml/min) | Mean Power (relative unit) | Power Ratio   |
|--------------------|----------------------------|---------------|
| 129 $\pm 2$        | 156 $\pm 51$               | 5.8 $\pm 1.4$ |
| 254 $\pm 5$        | 84 $\pm 60$                | 4.7 $\pm 1.1$ |
| 509 $\pm 6$        | 31 $\pm 19$                | 3.5 $\pm 1.0$ |
| 753 $\pm 5$        | 22 $\pm 9$                 | 2.9 $\pm 0.9$ |
| 1006 $\pm 3$       | 16 $\pm 5$                 | 2.2 $\pm 0.5$ |
| 1257 $\pm 2$       | 11 $\pm 4$                 | 1.9 $\pm 0.5$ |
| 1505 $\pm 7$       | 9 $\pm 2$                  | 1.7 $\pm 0.3$ |

TABLE II

MEAN SHEAR RATE ACROSS THE TUBE ESTIMATED FROM (6), AND PARAMETERS  $v_{\max}$  AND  $n$  OF THE MODEL FOR VALUES OF THE MEAN FLOW RATE BETWEEN 129 AND 1505 ml/min. ALL RESULTS ARE EXPRESSED IN TERM OF MEAN  $\pm 1$  STANDARD DEVIATION. THE FLOW RATES WERE MEASURED WITH AN ELECTROMAGNETIC BLOOD FLOWMETER. ALL MEASUREMENTS WERE REPEATED OVER SIX EXPERIMENTS WITH THE EXCEPTION OF THE RESULTS AT 1505 ml/min, SINCE ONLY THREE EXPERIMENTS WERE AVAILABLE

| Flow Rate (ml/min) | Mean Shear Rate Across the Tube ( $s^{-1}$ ) | $v_{\max}$ (cm/s) | $n$             |
|--------------------|--|-------------------|-----------------|
| 129                | 5.7 $\pm 0.6$                                | 2.4 $\pm 0.3$     | 2.8 $\pm 0.1$   |
| 254                | 11 $\pm 3$                                   | 5 $\pm 1$         | 2.6 $\pm 0.2$   |
| 509                | 24 $\pm 7$                                   | 11 $\pm 3$        | 2.5 $\pm 0.2$   |
| 753                | 34 $\pm 4$                                   | 15 $\pm 2$        | 2.5 $\pm 0.1$   |
| 1006               | 47 $\pm 8$                                   | 21 $\pm 3$        | 2.5 $\pm 0.1$   |
| 1257               | 61 $\pm 7$                                   | 27 $\pm 3$        | 2.47 $\pm 0.09$ |
| 1505               | 74 $\pm 7$                                   | 33 $\pm 3$        | 2.39 $\pm 0.05$ |

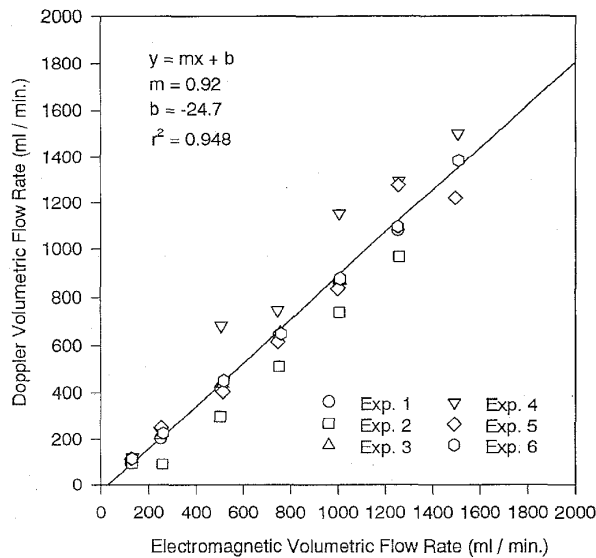


Fig. 6. First-order least square relationship between the Doppler volumetric flow rate and the flow rate measured with the electromagnetic flowmeter.

presents the mean shear rate across the tube estimated from (6) as well as parameters  $v_{\max}$  and  $n$  used in the Doppler volumetric flow evaluation. As shown in Table II and also in Fig. 5, a blunter velocity profile associated with the non-Newtonian property of porcine whole blood was obtained when reducing the flow rate from 1505 ml/min ( $n = 2.4$ ) to 129 ml/min ( $n = 2.8$ ).

#### H. Shear Rate and Shear Stress Dependences of Red Blood Cell Aggregation

The shear rate dependence of red blood cell aggregation was determined for the six porcine whole blood experiments. The results of Fig. 7 show a good reproducibility among experiments. Three zones characterized each curve: 1) a zone with a rapid reduction of the Doppler power between approximately 1 and 5  $s^{-1}$ , 2) an elbow around 5 to 10  $s^{-1}$ , and 3) a zone with a very slow reduction of the power beyond 10  $s^{-1}$ . An example from one experiment of the Doppler power as a function of the shear stress is shown in Fig. 8. It is clear from this figure that

the size of the aggregates was significantly reduced for shear stress ranging between 0.25 to 2  $\text{dyn/cm}^2$ . The reduction of the size of the aggregates for shear stress higher than 2  $\text{dyn/cm}^2$  was less important.

#### IV. DISCUSSION

As shown in Figs. 3 and 5, the accuracy of the experimental measurements of the Doppler frequency shift (velocity) was very good since no scattering around the fitted power law model was observed. The coefficient of determination  $r^2$  between the experimental and theoretical velocities was higher than 0.99 for all experiments. As shown in Fig. 6, some variance in the volumetric flow estimates was present. Part of the variance can be attributed to the Doppler method. It is also possible that improper cleaning of the electromagnetic probe between experiments or contamination of the electrode within an experiment have induced some variations. As also shown in Fig. 6, the Doppler method underestimated by 8% the volumetric flow measured with the electromagnetic flowmeter. This underestimation can be attributed to an error in the flow angle determination, a shift in the beam-to-vessel axis, or an underestimation of the radius of the tube. Picot and Embree [34] found that the largest source of uncertainty in the volume flow estimate was associated with the measurement of the Doppler angle. They found 5% uncertainty per degree of error in the flow angle determination. Since the angle between the tube axis and the axis of the transducer was measured visually with a goniometer, a small measurement error may have been present. A shift in the beam-to-vessel axis is also possible because the transducer was aligned visually. It is also possible that the tube radius could have been smaller than 0.635 cm because the thin-wall Kynar tubing was not perfectly circular. The effect of the underestimation of the volumetric flow on the shear rate estimates is unknown since the magnitude of this error was not quantified.

#### A. Effect of the Shear Rate on Blood Echogenicity

Very little data is available in the literature to compare with our results. In the steady flow study by Sigel *et al.* [9], the echogenicity of blood measured at the center of the tube at 10 MHz dropped exponentially with the mean shear rate estimated

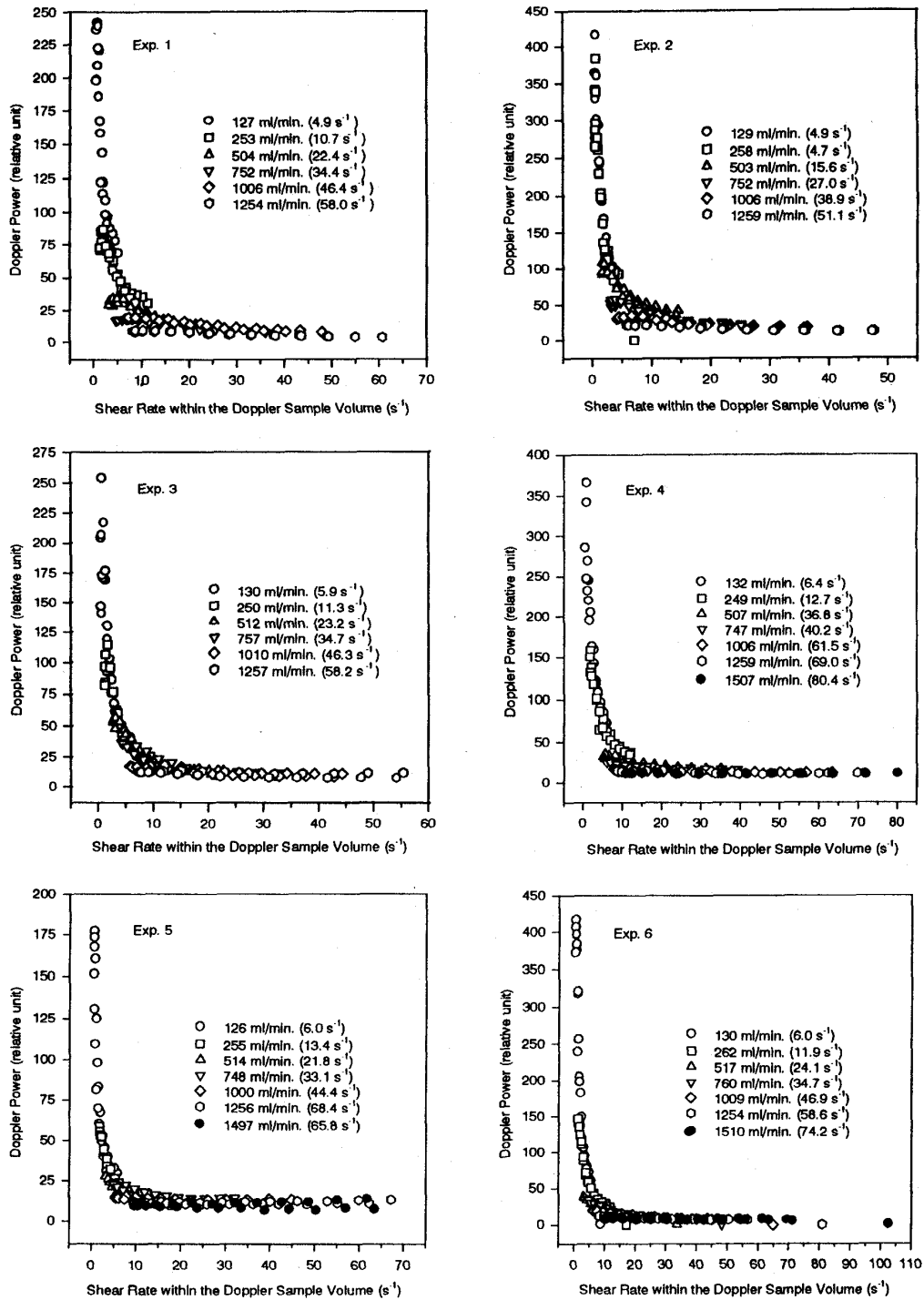


Fig. 7. Doppler power as a function of the mean shear rate within the Doppler sample volume for experiments one to six. The legends give the flow rate obtained with the electromagnetic flowmeter and the mean shear rate across the tube (numbers in parenthesis) estimated from (6).

assuming Poiseuille flow. In the present study, similar power variations were observed in Fig. 7. However, a meticulous comparison of our results with those in [9] is difficult because different methods were used to measure the echogenicity and the shear rate.

An interesting study relating the B-mode blood echogenicity at 7 MHz to the shear rate was reported by Shehada *et al.* [22]. The objective of this study was to better understand the black hole phenomenon observed at the center of large diameter tubes under very low shear rate conditions [35]. For

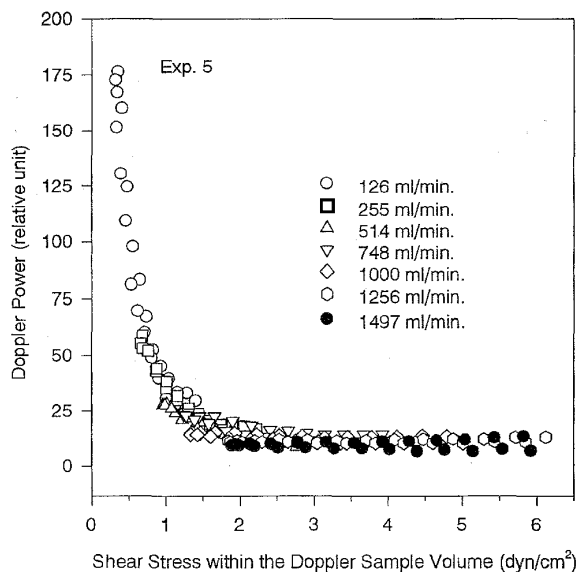


Fig. 8. Example from one experiment of the relationship between the Doppler power and the mean shear stress acting on the red cells within the Doppler sample volume. The legend gives the flow rate obtained with the electromagnetic flowmeter.

each position  $r$  across the tube (see [22]), the echogenicity was compared to the shear rate  $\gamma(r)$  estimated using (5). The actual shear rate within the ultrasonic sample volume was not estimated. The echogenicity increased when increasing the shear rate from 0.0001 to approximately  $1 \text{ s}^{-1}$ . At shear rates between 1 and  $10 \text{ s}^{-1}$ , the echogenicity dropped regularly with no change in the slope of the curve. In the present study, the slope changed significantly between approximately 5 and  $10 \text{ s}^{-1}$  (see Fig. 7). This difference between the results of both studies can be attributed to differences in the hematocrit (28% and 40%), transmitted frequency (7 MHz and 10 MHz), and to the possible overestimation of the shear rate in Shehada's study [22]. For instance, it is believed, based on our results, that an overestimation may have occurred due to the absence of weighting of the shear rate  $\gamma(r)$  by a function describing the radial ultrasonic beam power pattern (see the method described in Fig. 2). For high shear rates close to the wall of the tube, ignoring the radial beam power pattern probably resulted in an overestimation of the shear rates, while near the center of the tube, the low shear rates were perhaps underestimated.

Shehada *et al.* [22] also compared echogenicity as a function of the shear rate to erythrocyte sedimentation rates obtained by Copley *et al.* (see Fig. 6 of Shehada's paper). Good matching was obtained between the results of both studies. However, Copley *et al.* predicted maximum aggregation at a shear rate of  $0.1 \text{ s}^{-1}$  while Shehada *et al.* found maximum echogenicity around  $1 \text{ s}^{-1}$ . This observation also suggests that the shear rate may have been overestimated in Shehada's study. Other important factors that should however be considered are the hematocrit and the blood species difference between both studies. Shehada *et al.* used porcine whole blood at 28% hematocrit while Copley *et al.* studied human blood at hematocrits between 38 and 44%. In a study by Chien [36], the

aggregation was maximum at  $0.5 \text{ s}^{-1}$  for normal human red cells suspended, at 45% hematocrit, in a dextran 80 solution at a concentration of 4 g/100 ml. This suggests that the presence of bridging macromolecules may also affect the shear rate at which the maximum aggregation occurs.

### B. Comparison with the Results Obtained with the Erythro-Aggregameter

In the present study, the partial dissociation shear rates of the six porcine whole blood samples at 40% hematocrit and room temperature were found to be within the range of  $42 \pm 8 \text{ s}^{-1}$ . Using the same type of aggregameter, partial dissociation shear rates between 47 and  $65 \text{ s}^{-1}$  were obtained with normal human blood at 40% hematocrit and  $37^\circ\text{C}$  [37]. The use of porcine whole blood at room temperature thus slightly underestimated the cohesion forces of normal human erythrocytes.

The dissociation shear rates measured with the erythro-aggregameter are empirically extrapolated from the variation of the scattered light intensity (780 nm) as a function of the shear rates. The scattered light depends on the area, disaggregation and orientation of the red cells [29]. It is clear that ultrasound backscattering and light scattering do not provide the same type of information since the ultrasound backscattered power is principally a function of the volume square of the scatterers. Consequently, the direct comparison of the results of both methods is not straightforward. Using Couette flow and light reflectivity measurements at room temperature, Snabre *et al.* [38] found a monotonical decrease in the reflectivity index when the shear rate was raised above  $1 \text{ s}^{-1}$ , indicating a progressive shear-induced dispersion of the rouleaux into smaller ones. A critical shear stress value of  $2.5 \text{ dyn/cm}^2$  was measured in this last study with normal erythrocytes suspended in a saline solution of dextran 80. In the present study, critical shear stress values around  $2 \text{ dyn/cm}^2$  were obtained (see Fig. 8). Further work using blood with different aggregation tendencies will be necessary to compare the light scattering and ultrasound backscattering methods.

### C. Influence of the Structure of the Red Blood Cell Aggregates on the Doppler Power

Few experimental methods can allow the study of the shear rate or shear stress dependences of red cell aggregation. By making a cone-plate viscometer transparent, direct microscopic observations of normal human blood at shear rates from 5.8 to  $230 \text{ s}^{-1}$  were reported [39]. At the lowest shear rate, three-dimensional cluster of red cells and no typical rouleaux were distinguished for normal hematocrit and  $37^\circ\text{C}$ . By increasing the shear rate, the size of the aggregates decreased and individual red cells were observed at shear rates higher than  $46 \text{ s}^{-1}$ . The rheogram (the dynamic viscosity measured with a Couette viscometer as a function of the shear rate) was used to speculate on the structure of red cell aggregation [40]. Three regions of the rheogram were defined: region A which corresponds to shear rates between 0.05 and  $1 \text{ s}^{-1}$ , region B that refers to shear rates between 1 and  $20 \text{ s}^{-1}$ , and region C for shear rates higher than  $20 \text{ s}^{-1}$ . In region A, the red cells were believed to be organized in complex three-dimensional

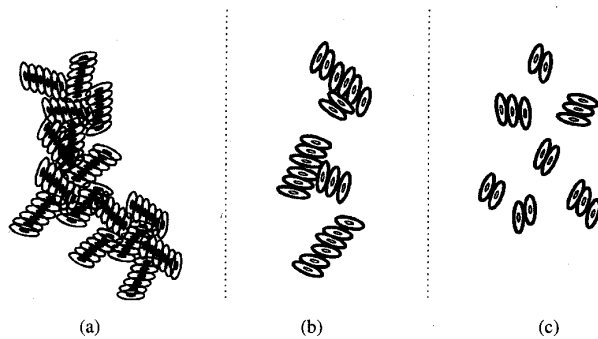


Fig. 9. Schematic representation of the structure of the red blood cell aggregates under three different shear flow conditions. (a) Shows the aggregate structure for shear rates between 1 and  $5 \text{ s}^{-1}$  (shear stresses between 0.25 and  $1 \text{ dyn/cm}^2$ ), (b) for shear rates between 5 to  $10 \text{ s}^{-1}$  (1 to  $2 \text{ dyn/cm}^2$ ), and (c) for shear rates higher than  $10 \text{ s}^{-1}$  ( $2 \text{ dyn/cm}^2$ ).

networks or individual rouleaux; in region B, an equilibrium was speculated between the aggregation and disaggregation of red cells; while in region C, the red cells were expected to be dispersed and oriented with the flow.

These studies on the structure of the aggregates are used here to propose an explanation of the results of Figs. 7 and 8. The rapid reduction of the Doppler power between approximately 1 and  $5 \text{ s}^{-1}$  ( $0.25$  to  $1 \text{ dyn/cm}^2$ ) is believed to be associated to the breaking of large three-dimensional networks of red cells. The transition around 5 to  $10 \text{ s}^{-1}$  ( $1$  to  $2 \text{ dyn/cm}^2$ ) is hypothesized to be due to the dissociation of small networks or rouleaux of red cells. The small reduction of the Doppler power for shear rates higher than  $10 \text{ s}^{-1}$  (shear stress  $> 2 \text{ dyn/cm}^2$ ) may be the result of the separation of small rouleaux of a few red cells. Since the energy needed to break large three-dimensional structures is certainly much smaller than the one necessary to disrupt small rouleaux, most variations of the Doppler power were observed within a small range of shear rate or shear stress. Fig. 9 illustrates our hypotheses on the structure of the aggregates under shear flow.

## V. CONCLUSION

It has been demonstrated that power Doppler ultrasound is a sensitive and reproducible technique to study the dynamics of red blood cell aggregation under steady flow. The variation of the Doppler power across the tube suggested that larger aggregates are around the center of the tube. An hypothesis concerning the effect of the shear conditions on the structure of the red blood cell aggregates was proposed. The variation of the Doppler power as a function of the shear rate or shear stress showed three specific regions: 1) a rapid reduction of the power that was postulated to be associated with the disruption of large three-dimensional aggregates, 2) a zone with a smaller reduction of the power probably due to the dissociation of large rouleaux, and 3) a region with a low variation of the power related presumably to the separation of small rouleaux of a few red cells.

## ACKNOWLEDGMENT

The authors gratefully acknowledge L. Allard for reviewing the manuscript. They would also like to thank L. Allard and Dr.

M. Bertrand of the Institute of Biomedical Engineering, Ecole Polytechnique, University of Montreal for their constructive suggestions.

## REFERENCES

- [1] R. Skalak, "Aggregation and disaggregation of red blood cells," *Biorheol.*, vol. 21, pp. 463-476, 1984.
- [2] R. W. Samsel and A. S. Perelson, "Kinetics of rouleau formation—II: Reversible reactions," *Biophys. J.*, vol. 45, no. 4, pp. 805-824, 1984.
- [3] S. M. Razavian, M. Del Pino, A. Simon, and J. Levenson, "Increase in erythrocyte disaggregation shear stress in hypertension," *Hypertension*, vol. 20, pp. 247-252, 1992.
- [4] F. Zannad, P. Voisin, F. Brunotte, J. F. Bruntz, J. F. Stoltz, and J. M. Gilgenkrantz, "Haemorheological abnormalities in arterial hypertension and their relation to cardiac hypertrophy," *J. Hypertension*, vol. 6, no. 4, pp. 293-297, 1988.
- [5] F. J. Neumann, H. A. Katus, E. Hoberg, P. Roebuck, M. Braun, H. M. Haupt, H. Tillmanns, and W. Kübler, "Increased plasma viscosity and erythrocyte aggregation: Indicators of an unfavorable clinical outcome in patients with unstable angina pectoris," *Br. Heart J.*, vol. 66, pp. 425-430, 1991.
- [6] J. F. Stoltz and M. Donner, "Hemorheology: Importance of erythrocyte aggregation," *Clin. Hemorheol.*, vol. 7, no. 1, pp. 15-23, 1987.
- [7] J. F. Stoltz, *Hémorhéologie et agrégation érythrocytaire. Applications cliniques. Troisième symposium international*, 1st ed. Versailles: Éditions Médicales Internationales, 1994.
- [8] K. K. Shung and J. M. Reid, "Ultrasonic instrumentation for hematology," *Ultrason. Imag.*, vol. 1, pp. 280-294, 1979.
- [9] B. Sigel, J. Machi, J. C. Beitler, J. R. Justin, and J. C. U. Coelho, "Variable ultrasound echogenicity in flowing blood," *Sci.*, vol. 218, pp. 1321-1323, 1982.
- [10] S. Beppu, Y. Nimura, H. Sakakibara, S. Nagata, Y. D. Park, S. I. Izumi, M. Ueoka, Y. Masuda, and I. Nakasone, "Smoke-like echo in the left atrial cavity in mitral valve disease: Its features and significance," *J. Am. Coll. Cardiol.*, vol. 6, no. 4, pp. 744-749, 1985.
- [11] R. Erbel, H. Stern, W. Ehrenthal, G. Schreiner, N. Treese, G. Krämer, M. Thelen, P. Schweizer, and J. Meyer, "Detection of spontaneous echocardiographic contrast within the left atrium by transesophageal echocardiography: Spontaneous echocardiographic contrast," *Clin. Cardiol.*, vol. 9, pp. 245-252, 1986.
- [12] X. F. Wang, L. Liu, T. O. Cheng, Z. A. Li, Y. B. Deng, and J. E. Wang, "The relationship between intracardiovascular smoke-like echo and erythrocyte rouleaux formation," *Am. Heart J.*, vol. 124, no. 4, pp. 961-965, 1992.
- [13] A. Merino, P. Hauptman, L. Badimon, J. J. Badimon, M. Cohen, V. Fuster, and M. Goldman, "Echocardiographic 'Smoke' is produced by an interaction of erythrocytes and plasma proteins modulated by shear forces," *J. Am. Coll. Cardiol.*, vol. 20, no. 7, pp. 1661-1668, 1992.
- [14] J. J. Hwang, F. N. Ko, Y. H. Li, H. M. Ma, G. J. Wu, H. Chang, S. M. Wang, J. T. Schie, Y. Z. Tseng, P. Kuan, C. M. Teng, and W. P. Lien, "Clinical implications and factors related to left atrial spontaneous echo contrast in chronic nonvalvular atrial fibrillation," *Cardiol.*, vol. 85, pp. 69-75, 1994.
- [15] T. Kallio and A. Alanen, "A new ultrasonic technique for quantifying blood echogenicity," *Investigat. Radiol.*, vol. 23, pp. 832-835, 1988.
- [16] Y. W. Yuan and K. K. Shung, "Ultrasonic backscatter from flowing whole blood—I: Dependence on shear rate and hematocrit," *J. Acoust. Soc. Am.*, vol. 84, no. 1, pp. 52-58, 1988.
- [17] ———, "Ultrasonic backscatter from flowing whole blood—II: Dependence on frequency and fibrinogen concentration," *J. Acoust. Soc. Am.*, vol. 84, no. 4, pp. 1195-1200, 1988.
- [18] S. Y. Kim, I. F. Miller, B. Sigel, P. M. Consigny, and J. Justin, "Ultrasonic evaluation of erythrocyte aggregation dynamics," *Biorheol.*, vol. 26, pp. 723-736, 1989.
- [19] E. G. Yamada, P. J. Fitzgerald, K. Sudhir, V. K. Hargrave, and P. G. Yock, "Intravascular ultrasound imaging of blood: The effect of hematocrit and flow on backscatter," *J. Am. Soc. Echocardiogr.*, vol. 5, pp. 385-392, 1992.
- [20] K. K. Shung, G. Cloutier, and C. C. Lim, "The effects of hematocrit, shear rate, and turbulence on ultrasonic Doppler spectrum from blood," *IEEE Trans. Biomed. Eng.*, vol. 39, no. 5, pp. 462-469, 1992.
- [21] G. Cloutier and K. K. Shung, "Study of red cell aggregation in pulsatile flow from ultrasonic Doppler power measurements," *Biorheol.*, vol. 30, no. 5/6, pp. 443-461, 1993.
- [22] R. E. N. Shehada, R. S. C. Cobbold, and L. Y. L. Mo, "Aggregation effects in whole blood: Influence of time and shear rate measured using

- ultrasound," *Biorheol.*, vol. 31, no. 1, pp. 115-135, 1994.
- [23] M. Boynard, J. C. Lelievre, and R. Guillet, "Aggregation of red blood cells studied by ultrasound backscattering," *Biorheol.*, vol. 24, pp. 451-461, 1987.
- [24] M. Boynard and J. C. Lelievre, "Size determination of red blood cell aggregates induced by dextran using ultrasound backscattering phenomenon," *Biorheol.*, vol. 27, pp. 39-46, 1990.
- [25] H. Hammi, P. Perrotin, R. Guillet, and M. Boynard, "Determination of red blood cell aggregation in young and elderly subjects evaluated by ultrasound: Influence of dihydroergocryptine mesylate," *Clin. Hemorheol.*, vol. 14, no. 1, pp. 117-126, 1994.
- [26] K. K. Shung and G. A. Thieme, *Ultrasonic Scattering in Biological Tissues*, 1st ed. Boca Raton, FL: CRC, 1993.
- [27] B. Sigel, J. Machi, J. C. Beitler, and J. R. Justin, "Red cell aggregation as a cause of blood-flow echogenicity," *Radiol.*, vol. 148, pp. 799-802, 1983.
- [28] X. D. Weng, G. Cloutier, P. Pibarot, and L. G. Durand, "Animal blood models simulating normal, hypo and hyperaggregating human red cells," in *Proc. 9th Int. Congress Biorheol.*, 32, no. 2/3, 1995, pp. 218-219.
- [29] M. Donner, M. Siadat, and J. F. Stoltz, "Erythrocyte aggregation: Approach by light scattering determination," *Biorheol.*, vol. 25, pp. 367-375, 1988.
- [30] L. Hatle and B. Angelsen, *Doppler Ultrasound in Cardiology. Physical principles and clinical applications*, 2nd ed. Philadelphia, PA: Lea & Febiger, 1985.
- [31] D. A. Christensen, *Ultrasonic Bioinstrumentation*, 1st ed. New York: Wiley, 1988.
- [32] F. J. Walburn and D. J. Schneck, "A constitutive equation for whole human blood," *Biorheol.*, vol. 13, pp. 201-210, 1976.
- [33] A. R. Selfridge, "Approximate material properties in isotropic materials," *IEEE Trans Sonics Ultrason.*, vol. 32, no. 3, pp. 381-394, 1985.
- [34] P. A. Picot and P. M. Embree, "Quantitative volume flow estimation using velocity profiles," *IEEE Trans Ultrason. Ferroelec. Freq. Cont.*, vol. 41, no. 3, pp. 340-345, 1994.
- [35] Y. W. Yuan and K. K. Shung, "Echogenicity of whole blood," *J. Ultrasound Med.*, vol. 8, pp. 425-434, 1989.
- [36] S. Chien, "Electrochemical interactions between erythrocyte surfaces," *Thrombosis Res.*, vol. suppl. II, no. 8, pp. 189-202, 1976.
- [37] B. Pignon, D. Jolly, G. Potron, B. Lartigue, J. P. Vilque, P. Nguyen, J. C. Etienne, and J. F. Stoltz, "Erythrocyte aggregation—Determination of normal values: Influence of age, sex, hormonal state, oestrogenic treatment, haematological parameters and cigarette smoking," *Nouv. Rev. Fr. Hematol.*, vol. 36, pp. 431-439, 1994.
- [38] P. Snabre, M. Bitbol, and P. Mills, "Cell disaggregation behavior in shear flow," *Biophys. J.*, vol. 51, pp. 795-807, 1987.
- [39] H. Schmid-Schönbein, P. Gachtgens, and H. Hirsch, "On the shear rate dependence of red cell aggregation *in vitro*," *J. Clin. Invest.*, vol. 47, pp. 1447-1454, 1968.
- [40] C. Lacombe and J. C. Lelievre, "Interprétation des rhéogrammes: relations avec l'agrégation et la déformabilité érythrocytaire," in *Hémorhéologie et agrégation érythrocytaire*, J. F. Stoltz, Ed. Paris: Éditions Médicales Internationales, 1986, pp. 33-46.



**Guy Cloutier** (S'89-M'90) obtained the B.Eng. degree in electrical engineering from the Université du Québec à Trois-Rivières in 1984 and the M.Sc. and Ph.D. degrees in biomedical engineering from the École Polytechnique, Université de Montréal in 1986 and 1990, respectively.

Between 1990 and 1992, he worked in collaboration with Dr. K. Kirk Shung at the Laboratory of Medical Ultrasonics, Bioengineering Program, the Pennsylvania State University, University Park, as a Postdoctoral Research Fellow of the Natural Sciences and Engineering Research Council of Canada. He is currently Associate Researcher at the Laboratory of Biomedical Engineering of the Institut de recherches cliniques de Montréal, Research Assistant Professor at the Department of Medicine of the Université de Montréal, and Adjunct Researcher at the Institute of Biomedical Engineering of the École Polytechnique de Montréal. His research interests are in blood biorheology, hemodynamics, Doppler ultrasound, and ultrasonic tissue characterization.

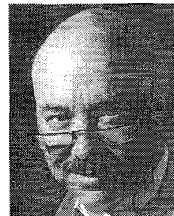
Dr. Cloutier is the recipient of a research scholarship from the Fonds de la Recherche en Santé du Québec.



Her main research interest is in Doppler ultrasonography to study erythrocyte aggregation.

**Zhao Qin** was born in Beijing, China in 1956. She received the masters degree in biomedical sciences from Beijing Second Medical College, Beijing, China in 1989.

From 1983 to 1992, she worked as a Teaching Assistant at the Department of Biomedical Engineering of Beijing Second Medical College. Since 1994, she has been with the Laboratory of Biomedical Engineering of the Clinical Research Institute of Montreal, Québec, Canada, where she is now pursuing the M.Sc. degree in Biomedical Sciences.



**Louis-Gilles Durand** (M'78-SM'85) received the B.Sc., M.Sc., and Ph.D. degrees in electrical engineering from the École Polytechnique, University of Montreal, Canada, in 1975, 1979, and 1983, respectively.

He is presently Director of the Biomedical Engineering Laboratory at the Institut de Recherches Cliniques de Montreal (IRCM), Research Professor in the Department of Medicine of the University of Montreal, Adjunct Professor at the Institute of Biomedical Engineering, Ecole Polytechnique and University of Montreal, and Adjunct Professor in the Department of Electrical Engineering at McGill University, Montreal. His current research interests are the development of noninvasive methods for the detection and quantification of cardiac valve dysfunction by computer analysis of heart sounds and Doppler blood flow velocity, development of a noninvasive method for the quantification of multiple stenoses of the lower limb arterial tree by computer analysis of Doppler blood flow velocity, and development of medical instrumentation.



**Beng Ghee Teh** was born in George Town, Penang, Malaysia, in 1971. He received the B.Eng. degree in electrical engineering from McGill University, Montreal, Québec, Canada in 1994. He is currently pursuing the M. Eng. degree in electrical engineering at McGill University and the Clinical Research Institute of Montreal. His research interest is in digital signal processing, especially in the area of medical ultrasound.